

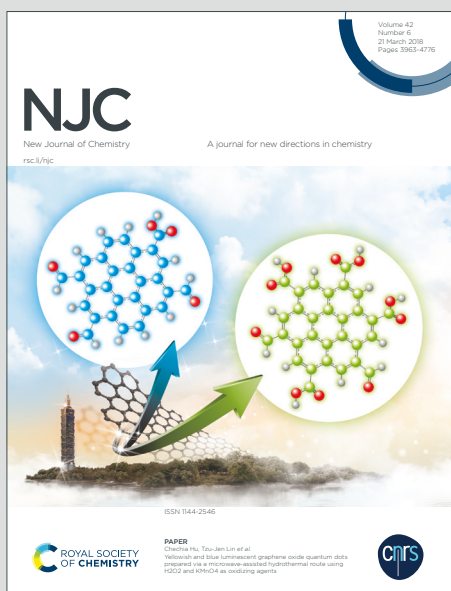
NJC

New Journal of Chemistry

Accepted Manuscript

A journal for new directions in chemistry

This article can be cited before page numbers have been issued, to do this please use: K. S. Sharma, A. K. Dubey, A. S. Kojiam, C. Kumar, A. Ballal, S. Mukherjee, P. P. Phadnis and R. K. Vatsa, *New J. Chem.*, 2020, DOI: 10.1039/C9NJ05989J.



This is an Accepted Manuscript, which has been through the Royal Society of Chemistry peer review process and has been accepted for publication.

Accepted Manuscripts are published online shortly after acceptance, before technical editing, formatting and proof reading. Using this free service, authors can make their results available to the community, in citable form, before we publish the edited article. We will replace this Accepted Manuscript with the edited and formatted Advance Article as soon as it is available.

You can find more information about Accepted Manuscripts in the [Information for Authors](#).

Please note that technical editing may introduce minor changes to the text and/or graphics, which may alter content. The journal's standard [Terms & Conditions](#) and the [Ethical guidelines](#) still apply. In no event shall the Royal Society of Chemistry be held responsible for any errors or omissions in this Accepted Manuscript or any consequences arising from the use of any information it contains.

1
2
3
4
5
6
7
8
9
10
11
12
13
14
15
16
17
18
19
20
21
22
23
24
25
26
27
28
29
30
31
32
33
34
35
36
37
38
39
40
41
42
43
44
45
46
47
48
49
50
51
52
53
54
55
56
57
58
59
60

View Article Online
DOI: 10.1039/C9NJ05989J

Synthesis of 2-deoxy-D-glucose coated Fe₃O₄ nanoparticles for applications in targeted delivery of Pt(IV) prodrug of cisplatin - a novel approach in chemotherapy

K. Shitaljit Sharma^a, Akhil K. Dubey^b, Arunkumar S. Koijam^c, Chandan Kumar^c, Anand Ballal^d, Sudip Mukherjee^e, Prasad P. Phadnis^{a, f*}, Rajesh K. Vatsa^{a, f*}

^a Chemistry Division, Bhabha Atomic Research Centre, Mumbai-400 085, India, Email: phadnisp@barc.gov.in, Tel.: +91 22 2559 2229; rkvatsa@barc.gov.in; Tel.: +91 22 2559 2438, Fax: +91 22 2550 5151

^b Bio-Organic Division, Bhabha Atomic Research Centre, Mumbai-400 085, India

^c Radiopharmaceuticals Division, Bhabha Atomic Research Centre, Mumbai-400 085, India

^d Molecular Biology Division, Bhabha Atomic Research Centre, Mumbai-400 085, India

^e UGC-DAE Consortium for Scientific Research, Mumbai Centre, Mumbai-400 085, India

^f Homi Bhabha National Institute, Anushaktinagar, Mumbai-400 094, India

Abstract

Water soluble Pt(IV) prodrug of cisplatin was synthesized by oxidation of cisplatin followed by treatment with succinic anhydride to achieve easily reducible ester linkage at axial positions which was evidenced from cyclic voltammetric analyses. Because of this modification Pt(IV) prodrug has achieved better physicochemical and pharmacological properties like water solubility and reduced toxicity for normal (non-cancerous) CHO cells respectively, as compared to cisplatin. Later, this Pt(IV) prodrug was loaded on 2-deoxy-D-glucose (2DG) functionalized over silica coated Fe₃O₄ magnetic nanoparticles (MNPs) to achieve a desired formulation. It exhibited the potency as evidenced from the cytotoxicity

1
2
3 evaluation against MCF-7 human breast cancer cell lines ($IC_{50} \sim 14 \mu M$). This encouraged to
4 further study for the percentage viability, apoptosis and cell death evaluations on MCF-7,
5 Colo-205 and CHO cells by flow cytometry. It displayed the cytotoxic potency of
6 formulation to cancer cells, Colo-205 and MCF-7 (22-30% apoptosis) while the parent
7 formulation is non-toxic to non-cancerous, CHO cell lines (3% apoptosis) as compared to
8 cisplatin. It revealed that, the formulation is worthy to increase the efficacy of killing cancer
9 cells equivalent to cisplatin. Additionally the FITC labeled MNPs coated with 2DG exhibited
10 efficient cell uptake and fast internalization (within 3 h) accumulating mainly in cytoplasm
11 and at cell surface. Besides this, the formulation exhibited heating efficacy anticipating its
12 possible application for hyperthermia also. These results are indicating possible utility of
13 formulation for site specific delivery of Pt(IV) prodrug of cisplatin.
14
15
16
17
18
19
20
21
22
23
24
25
26
27
28
29
30
31
32
33
34
35
36
37
38
39
40
41
42
43
44
45
46
47
48
49
50
51
52
53
54
55
56
57
58
59
60

Keywords: Fe_3O_4 MNPs, 2-deoxy-D-glucose, Pt(IV) prodrug of cisplatin, Warburg effect

1. Introduction

Globally, platinum based anticancer drugs, especially cisplatin, are widely used for treatment of cancers like carcinomas, lymphomas, sarcomas and malignant tumors *etc.* [1-3]. However, they exhibit inherent undesired dose-limiting toxic side effects because of non-selective side reactions with methallothionein and thiols like glutathione which leads to their deactivation, lesser bioavailability, short retention time in bloodstream and acquiring of resistance [4, 5]. Many approaches are being carried out to improve their therapeutic index such as introduction of stable ligands or changing the oxidation state of Pt metal ion. As a result of these studies, it has been recognized that the octahedral shaped Pt(IV) oxidation state which can be reduced to the active cytotoxic Pt(II) form by cellular reductants, is a promising option for cancer treatment and referred as the Pt(IV) prodrug approach [6, 7]. Generally, Pt(IV) prodrug consists of two axial hydroxyl groups and through these groups,

1
2
3
4
5
6
7
8
9
10
11
12
13
14
15
16
17
18
19
20
21
22
23
24
25
26
27
28
29
30
31
32
33
34
35
36
37
38
39
40
41
42
43
44
45
46
47
48
49
50
51
52
53
54
55
56
57
58
59
60

variety of groups like lipophilic, fluorescence moieties [8] or drugs which act synergistically (adjunct) can be conjugated [9]. Moreover, the choice of axial ligands plays a crucial role to enhance the efficacy of a prodrug by allowing to reduce [10, 11] easily at cancer site or by introducing moieties which enhance cellular accumulation and uptake [12, 13]. The Pt(IV) based prodrugs of cisplatin, carboplatin, and oxaliplatin are being studied for potent anticancer activity [14]. The transfer of Pt(IV) prodrug from research to clinical modalities however needs to understand the cellular pathway and perform on-demand release of drug specifically to the tumor site using delivery vehicles. To achieve this goal, the researchers have designed and evaluated various drug delivery vehicles on basis of rationale like biocompatibility, non-toxicity to normal cells, water dispersibility, high drug loading capacity, usefulness in treatment evaluation by luminescence and imaging [15]. Eventually diverse drug delivery systems [16] like inorganic nanoparticles [17], metal-organic frameworks (MOFs) [18] and biodegradable polymer [19], protein, peptide [20], lipid-based [21] and dendrimers based [22] delivery systems were explored. Among these, inorganic nanoparticles have attracted considerable attention because of their excellent effects, which have been accomplished by use of nanoparticles like gold, iron oxide (Fe_3O_4), carbon nanotubes and mesoporous silica for delivery of Pt(IV) prodrug [23]. Out of these inorganic nanoparticles, iron oxide (Fe_3O_4) nanoparticles have been explored for their biocompatibility up to certain concentrations and superparamagnetic nature. Above these, Fe_3O_4 based nanoformulations are preferably employed as drug delivery vehicles as they can be localized at desired site with the help of an external magnet [24] or to kill cancer cells by using thermal energy released under an AC magnetic field (hyperthermia treatment) [25]. For better targeting, dispersibility and internalization, Fe_3O_4 magnetic nanoparticles are usually coated by various biologically active molecules like antibody, antigen, proteins and peptides *etc.* [26-28].

As cancer cells solely depend on glycolysis for energy and nutrient to survive and proliferate, use of 2DG which lacks a hydroxyl group at 2-position (C-2) as compared to D-glucose can inhibit glycolysis by blocking the conversion of 2-deoxy-D-glucose-6-phosphate to fructose-6-phosphate [29, 30].

In our present study, Fe₃O₄ magnetic nanoparticles were synthesized by thermolysis method using oleic acid as the capping agent and 1-octadecene as the solvent. As the synthesized Fe₃O₄ magnetic nanoparticles are easily dispersible in non-polar solvent but not in polar solvent like water, the Fe₃O₄ nanoparticles were coated with silica homogeneously to achieve water dispersibility [31-33] followed by functionalizing with amine functional groups. Later the amine functional groups were conjugated with 2-DG through thiourea linkage giving hydroxyl functional groups on the surface of the nanoparticles. Using these hydroxyl groups, Pt(IV) prodrug of cisplatin was loaded through the ester bond. To the best of our knowledge, the present formulation has been reported for the first time as it involved the linkage of 2DG by chemical bond. Here we are reporting synthesis of monodispersed Fe₃O₄ based nanoparticles coated with silica (SiO₂) and functionalized with poly(amidoamine) and 2DG for delivering Pt(IV) prodrug of cisplatin and evaluation of its cytotoxic activity against the CHO, Colo-205 and MCF-7 breast cancer cell lines, This result encouraged us to extend the studies to flow cytometric evaluation for percentage viability, apoptotic cells and dead cells. The results are reported herein.

2. Experimental

2.1. Materials and Methods

The chemicals and some solvents required for this study, *viz.*, ferric chloride, oleic acid, 1-octadecene, tetraethyl orthosilicate (TEOS), tetra-*n*-butylammonium bromide (TBAB), 3-aminopropyl trimethoxysilane (APTMS), methyl acrylate, ethylenediamine,

1
2
3 benzoyl chloride, zinc metal, Igepal-500, lithium bromide, hydrogen bromide (33%) in acetic acid, DOWEX-500 resins, 2-deoxy-D-glucose (2DG), D-glucose (DG), ammonium chloride,
4
5
6
7
8 acetic acid, hydrogen peroxide, succinic anhydride, potassium thiocyanate, N, N'-
9
10 dicyclohexylcarbodiimide (DCC), hydrazine hydrochloride, Concanavalin A (ConA),
11
12 Fluorescein isothiocyanate (FITC), 3-(4, 5-dimethylthiazolyl-2)-2, 5-diphenyltetrazolium
13
14 bromide (MTT), pyridine, dimethyl formamide (DMF), dimethyl sulfoxide (DMSO) *etc.*
15
16 were purchased from commercial sources (Sigma-Aldrich). Guava ViaCount reagent was
17
18 purchased from Luminex Corporation, USA. The 4', 6-diamidino-2-phenylindole (DAPI) was
19
20 purchased from Molecular Probes Inc., USA. All solvents were dried following the standard
21
22 procedure [34].
23
24

25
26
27 The Pt(IV) compound was purified by recrystallization in ethanol-water mixture at
28
29 room temperature. NMR spectra were recorded on the Agilent / Varian 600 MHz NMR
30
31 spectrometer with a Unity Inova console operating at 599.88 (^1H), 150.84 ($^{13}\text{C}\{^1\text{H}\}$) and
32
33 128.95 MHz ($^{195}\text{Pt}\{^1\text{H}\}$). The ^1H and $^{13}\text{C}\{^1\text{H}\}$ NMR chemical shifts were relative to internal
34
35 DMSO peak. The $^{195}\text{Pt}\{^1\text{H}\}$ NMR chemical shifts were relative to external Na_2PtCl_6 in D_2O
36
37 (δ 0 ppm). The powder X-ray diffraction (XRD) patterns were recorded on a Pan analytical
38
39 X'pert PRO X-ray diffractometer using $\text{Cu-K}\alpha$ radiation in the 2θ range of $10\text{-}70^\circ$ with step
40
41 size and time of 0.02° and 1.20 s, respectively. XRD patterns were analyzed by comparing
42
43 with reported data for the end member compositions (JCPDF) files. Magnetization
44
45 measurements were carried out on a vibrating sample magnetometer (VSM) coupled to a 9
46
47 Tesla physical property measurement system (PPMS) (Model: 6000, Quantum Design,
48
49 USA). The transmission electron microscopic (TEM) image was recorded on Libra-120 plus
50
51 TEM (Carl Zeiss, Germany) operated at 120 kV as the accelerating voltage. TEM images
52
53 were analyzed by using Image J software taking 100 nanoparticles statistically. The cyclic
54
55 voltammetric studies were performed potentiostatic control using Eco Chemie Potentiostat,
56
57
58
59
60

AUTOLAB-100 with the VA663 stand. Electrochemical impedance measurements were carried out using the frequency response analyzer (FRA) module attached with Autolab-100 potentiostat.

Cell culture experiments

CHO, Colo-205 and MCF-7 cell lines were obtained from the National Center for Cell Sciences (NCCS) Pune, India and cultured in DMEM supplemented with 10 % serum (Invitrogen CA, USA) and antibiotic/antimycotic solution. Cells were grown in humidified 5 % CO₂ atmosphere in incubator at 37 °C and passaged for every alternate day. The cytotoxicity of formulation was evaluated against human breast adenocarcinoma cell line (MCF-7) by MTT assay. The cell viability, apoptosis and cell death of different cancer and normal cell lines were evaluated by Guava flow cytometer (Luminex Corp. USA). The cell lines were treated with test formulations followed by Guava ViaCount reagent followed by evaluation with flow cytometer. The data was analyzed using guavaSoft 3.1.1 software. Internalization of MNPs-2DG-FITC with MCF-7 cells stained with DAPI was studied by visualizing image at 40x magnification using a fluorescence microscope (Axioplan, Carl-Zeiss, Germany).

2.2. Preparation of formulation

The formulation MNPs-Pt(IV) prodrug was synthesized in following steps.

2.2.1. Synthesis of Fe₃O₄ magnetic nanoparticles (MNPs) [35]

In a beaker containing ferric chloride (5 g, 30 mmol) dissolved in methanol (40 ml) and water (90 ml), oleic acid (31.13 ml, 27.86 g, 98.6 mmol) dissolved in petroleum ether (50 ml) was added and stirred vigorously. Later a solution of sodium hydroxide (3.94 g, 98.5 mmol) was added slowly to it. After stirring the reaction mixture for about 1 h, the formation of two phases was observed with clear and transparent lower aqueous phase. The upper organic layer was collected using a separating funnel. It was refluxed for 1 h and

concentrated *in vacuo*. The slurry of ferric oleate was obtained. Further the ferric oleate (2 g) and oleic acid (2 ml) were dissolved in 1-octadecene (15 ml) placed in a 150 ml three necked round bottom flask. After purging with argon gas for 10 min., the reaction mixture was heated at a rate of 4 °C per min until it reached to 320 °C. Heating was maintained at this temperature for 30 min and then cooled to room temperature. Oleic acid coated Fe₃O₄ MNPs were precipitated out by acetone and washed by dispersion and precipitation using hexane and acetone. The Fe₃O₄ MNPs were characterized by X-ray diffraction (XRD) patterns; 2θ in deg (°): 20, 35, 40, 55, 60 (Figure 1 A) which matched with the JCPDF: 771545 reported data files. Further the MNPs were characterized with vibrating sample magnetometer (VSM) and transmission electron microscopy (TEM).

2.2.2. Coating of MNPs by silica [36]

To oleic acid coated Fe₃O₄ MNPs (200 mg) dispersed in cyclohexane (400 ml), the Igepal-500 (2 g) was added and stirred for 20 min followed by addition of ammonia solution (500 μl) and TEOS (1.5 ml) over a period of 16 h. The reaction mixture was stirred further for 72 h and then (3-aminopropyl)trimethoxysilane (APTMS) (3 ml) was added to it. After stirring the reaction mixture further for 24 h, methanol (20 ml) was added and stirred for next 20 min. The methanol layer was separated and MNPs@SiO₂-NH₂ (800 mg) was collected by centrifugation. It was characterized by FT-IR spectroscopy (Figure 2 C). Further these MNPs were characterized with transmission electron microscopy (TEM).

2.2.3. Functionalization of the silica coated MNPs by PAMAM (MNPs-PAMAM)

To the MNPs@SiO₂-NH₂ (100 mg) dispersed in ethanol (10 ml), methyl acrylate (2 ml) was added at 0 °C and then stirred at 45 °C for 24 h. Then the reaction mixture was centrifuged and the nanoparticles were obtained. They were washed with ethanol for several times till there was no smell of methyl acrylate and then dispersed in ethanol (10 ml). Then

1
2
3 ethylenediamine (2 ml) was added to the dispersion at 0 °C and stirred at 45 °C for 24 h. The
4
5 nanoparticles were collected by centrifugation. The whole procedure was repeated two times.
6
7

8 **2.2.4. Functionalization of MNPs-PAMAM by 2-DG (MNPs-2DG)**

9
10 It was synthesized by reaction of MNPS-PAMAM loaded with 3, 4, 5-tri-O-benzoyl-
11
12 2-deoxyglycopyranosyl isothiocyanate (Suppl. Info.: Synthesis Procedures S 1: Glucose
13
14 precursor & Figures S 1 - S 10).
15

16
17 The MNPs-PAMAM (50 mg) were dispersed into dimethyl formamide (5 ml), to
18
19 which 3, 4, 5-tri-O-benzoyl-2-deoxyglycopyranosyl isothiocyanate (100 mg) was added and
20
21 stirred at 60 °C for 12 h. The nanoparticles were separated by centrifugation and washed with
22
23 acetone several times. Nanoparticles were again dispersed in methanol (5 ml) and cooled to 0
24
25 °C, followed by addition of hydrazine solution (20 ml, 30 % in water) and stirring for
26
27 overnight at room temperature. The particles were washed with water and followed by
28
29 methanol. The obtained nanoparticles were dried under the IR lamp. They are hence further
30
31 referred to MNPs-2DG.
32
33

34 **2.2.5. Quantification of 2DG on the surface of the MNPs-2DG**

35
36 The amount of 2DG on the surface of MNPs-2DG was confirmed by monitoring the
37
38 amount of sulphur generated in elemental analyses. Along with this, presence of 2DG
39
40 moieties on the surface of the nanoparticles was confirmed by treating the nanoparticles with
41
42 FITC labeled Con A and measuring the emission of the supernatant obtained after separating
43
44 the nanoparticles using an external magnetic field.
45
46
47
48

49 **2.2.6. Loading of Pt(IV) prodrug of cisplatin over MNPs-2DG**

50
51 It was performed in following steps.

52 **(i) Synthesis of Pt(IV) prodrug of cisplatin [37]**

53
54 The cisplatin, [PtCl₂(NH₃)₂] (0.135 g, 0.449 mmol) was dissolved in water (10 ml)
55
56 followed by treatment with aqueous solution of hydrogen peroxide (30 %). The reaction
57
58
59
60

1
2
3 mixture was warmed to 60 °C for 1 h and cooled to room temperature and stirred further for
4
5
6 overnight. The reaction mixture was concentrated *in vacuo*, filtered and washed with ethanol
7
8 for three times giving almost quantitative yields (0.146 g, 97%) of Pt(IV) prodrug of
9
10 cisplatin. The Pt(IV) prodrug was dissolved in dimethyl sulfoxide (5 ml) and succinic
11
12 anhydride (0.095 g, 0.077 ml, 0.945 mmol) was added and stirred for overnight at room
13
14 temperature. The solvent was evaporated by lyophilizer yielding a creamy compound which
15
16 was washed with acetone three times and then dried *in vacuo* to yield a solid compound
17
18 (0.207 g, 86%). At this stage the purity of prodrug was evaluated by HPLC system on a
19
20 reverse phase column using methanol-water (10:90 v/v) as mobile phase. It revealed
21
22 acceptable purity as evidenced from a single peak. It was characterized by NMR
23
24 spectroscopy. ¹H NMR in dms_o-d₆ δ: 2.36 (t, 8 H), 2.49 (t, 9 H), 6.44 (br, S, 13 H) ppm;
25
26 ¹³C{¹H} NMR in dms_o-d₆ δ: 30.2, 30.8, 174.2, 180.0 ppm; ¹⁹⁵Pt{¹H} NMR in dms_o-d₆ δ:
27
28 1220 ppm (Suppl. Info. Figures S 12-14).

29
30
31
32
33
34
35
36
37
38
39
40
41
42
43
44
45
46
47
48
49
50
51
52
53
54
55
56
57
58
59
60

(ii) Cyclic voltammetric studies for evaluation of reduction of Pt(IV) prodrug of cisplatin to cisplatin at pH 6.5 and 7.4 with various scan rates

The Pt(IV) prodrug of cisplatin was dissolved in PBS buffer (10 mM) and adjusted pH at 6.5 and 7.4 respectively. The 1 ml stock solution was diluted in 20 ml of distilled water and then the electrolytic measurements were performed. The cyclic voltammetric analyses of 1.0 mM Pt(IV) prodrug of cisplatin in PBS buffer solution at pH 6.5 and 7.4 were performed using Ag/AgCl electrode. The different scan rates viz., 10, 20, 30, 40, 50 mV.s⁻¹ were employed for these electrolytic studies.

(iii) Loading of Pt(IV) prodrug of cisplatin on MNPs-2DG (MNPs-Pt(IV) prodrug)

To the Pt(IV) prodrug of cisplatin (3 mg) dissolved in DMF (500 μl) at 0 °C, the N, N'-dicyclohexylcarbodiimide (1 mg per 10 ml in DMF; 1 equivalent) was added and stirred at room temperature for overnight. Then the MNPs-2DG (3 mg) dissolved in DMF (2 ml) was

added to it and stirred further for overnight. The mixture was centrifuged and the MNPs were separated and then washed with methanol (2 times) and acetone (2 times). Loading of Pt(IV) prodrug of cisplatin on the surface of the MNPs was confirmed by ICP-OES analysis.

Prior to loading, the Pt(IV) prodrug on nanoparticles the electrolytic studies were performed to assess the reduction of Pt(IV) prodrug of cisplatin to Pt(II) *i.e.*, cisplatin.

2.2.7. Evaluation of cytotoxicity of MNPs-Pt(IV) prodrug formulation against MCF-7 cell lines in vitro by MTT assay [38]

The MTT assay was performed in cell culture media. The cytotoxicity of cisplatin, MNPs-2DG and Pt(IV) prodrug loaded NPs *i.e.*, MNPs-Pt(IV) prodrug was evaluated *in vitro* against MCF-7 human breast cancer cell lines using MTT assay method. 10000 cells were plated in a 96 well plate and incubated for overnight in humidified incubator with 5 % CO₂. Stock solution of the test compound (10 mM) was prepared either in PBS or in 0.9 M saline solutions. The cells were exposed to various concentrations of the compounds (5, 10, 20 and 40 μM) for 48 h. After the exposure, MTT was added (10 μl from 5 mg / ml) and incubated for 4 h. The formazan crystals formed were dissolved in DMSO and absorbance was recorded at 590 nm in a microplate reader. Toxicity expressed as percentage cytotoxicity, was calculated by the following formula:

$$\text{Percentage cytotoxicity} = \frac{\text{Control}_{\text{abs}} - \text{Test}_{\text{abs}}}{\text{Test}_{\text{abs}}} \times 100$$

2.2.8. Estimation of percentage viable, apoptotic and dead cells by flow cytometer [39]

The evaluations were performed with CHO, Colo-205 and MCF-7 cell lines. In a typical experiment 1 x 10⁵ cells were plated in 12 well plates for overnight and 10 μM of cisplatin, Pt(IV) prodrug and corresponding amounts of MNPs-2DG, MNPs-Pt(IV) prodrug were added in each well and incubated for 48 h. All experiments were carried out in triplicate. After completion of incubation, cells were washed, trypsinized and Guava

ViaCount (Luminex Corp. USA) reagent was added in each well. The cells were analyzed by Guava Flow cytometer (Luminex Corp. USA). Percentage viable, apoptotic and dead cells were estimated for all the three cell lines. (Please see the details in Suppl. Info. Table S 1, Figures S 15-17).

2.2.9. Labeling of the nanoparticles with FITC [40]

Labeling of the MNPs with FITC was done by reacting amine groups present on the surface of the nanoparticles. To study internalization of the MNPs-2DG labeling with FITC was performed prior to the conjugation with 2DG. After labeling, the MNPs were washed with water two times by centrifugation and dialyzed using dialysis tubing in 0.1 M saline solution for two days with frequent change of medium.

2.2.10. Internalization study on MCF-7 cell lines [41]

For studying the intracellular uptake, MNPs-2DG were labeled with FITC, followed by testing its internalization efficacy in MCF-7 cells (protocol for FITC labeling is given in Section 2.2.9.). Briefly, MCF-7 cells (1×10^6) were seeded on glass cover slips for overnight at culture conditions, followed by treatment with MNP-2DG-FITC for 3 h. The cells were then washed with PBS, followed by fixing in 4% paraformaldehyde for 20 min. at room temperature (RT). The cells were further washed with PBS and mounted on slide using Prolong Gold mounting media containing DAPI (Molecular Probes, USA). The cells were visualized by fluorescence microscopy under 40 X magnification.

2.2.11 Hyperthermia studies [35, 42]

Induction heating of MNPs-2DG coated with 2-DG, was performed in plastic micro-centrifuge tube (1.5 ml) using AC magnetic field (Easy Heat 8310, Ambrell, UK) with 6 cm diameter (4 turns) coil. Particles (0.5-2 mg) suspended in 1 ml of distilled water were placed at the centre of coil and frequency was applied at 265 kHz.

3. Results and discussion

View Article Online
DOI: 10.1039/C9NJ05989J

In order to obtain the nano carrier for drug delivery, synthesis of Fe_3O_4 (magnetite) magnetic nanoparticles (MNPs) was initiated through thermal decomposition of ferric oleate. The reaction of $\text{FeCl}_3 \cdot 6\text{H}_2\text{O}$ in methanolic aqueous solution and oleic acid ($\text{C}_{17}\text{H}_{33}\text{COOH}$) solution in petroleum ether in basic medium at room temperature followed by reflux yielded ferric oleate. Its thermal decomposition in 1-octadecene at $320\text{ }^\circ\text{C}$ yielded the Fe_3O_4 nanoparticles [43]. They were characterized by powder X-ray diffraction (XRD) which revealed the cubic spinel phase of Fe_3O_4 (JCPDS PDF No. 771545) MNPs (Figure 1A) [44]. The broadening of a peak in a diffraction pattern reveals the small size of NPs. Hence the MNPs were characterized with more sensitive and superior tool of TEM which gives the direct (real space) visualization of NPs of very small size as well demonstrates morphological pattern [45]. The morphology of Fe_3O_4 MNPs was studied with TEM (Figure 1B) and observed to be monodispersed (uniform shape and size). The size of the nanoparticles was determined by statistical evaluation of 100 nanoparticles and was found to have 16 ± 1 nm cuboid nanoparticles. The magnetic properties of the Fe_3O_4 nanoparticles were studied by vibrating sample magnetometer (VSM) [46]. There is no coercivity (H_c) of the Fe_3O_4 nanoparticles at room temperature but coercivity (H_c) is observed when measured at 5 K (Figure 1C). This reveals that the synthesized nanoparticles are superparamagnetic at room temperature which is desired in theranostic [47], drug delivery [47] as well as hyperthermia [49]. The saturation magnetization of the nanoparticles was calculated by plotting M Vs $1/H$. The blocking temperature T_b (temperature at which superparamagnetism to ferrimagnetism transition takes place) was found out to be 190 K (Figure 1D).

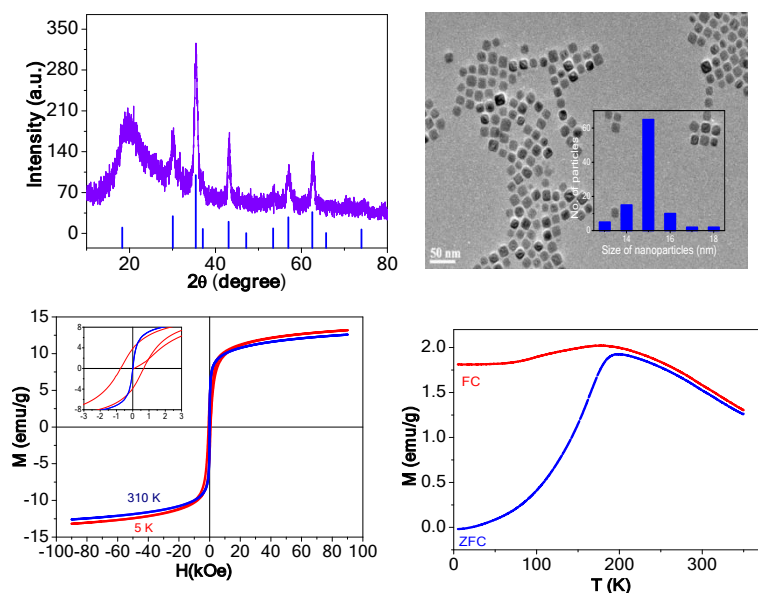


Figure 1. Characterization of the Fe_3O_4 MNPs by powder XRD (1A), TEM (1B) and vibrating sample magnetometer (VSM) (1C & 1D) respectively

The presence of oleic acid on these NPs renders them hydrophobic in nature. However, for better biocompatibility in health related applications [50]; hydrophilic MNPs [51] are preferred which is possible by surface modifications [52]. Hence the MNPs were coated with biocompatible silica by modified Stöber *et al.*, [53] method which produced $\text{Fe}_3\text{O}_4@\text{SiO}_2$ MNPs. They were characterized by powder X-ray diffraction (XRD) which revealed the presence of cubic spinel phase of Fe_3O_4 (JCPDF PDF no. 771545) and SiO_2 (JCPDF PDF no. 821576) in XRD pattern (Figure 2A) confirmed the formation of Fe_3O_4 and SiO_2 phases. Formation of the core shell $\text{Fe}_3\text{O}_4@\text{SiO}_2$ was further confirmed by observing TEM image (Figure 2B) due to the difference in refractive index of the shell (SiO_2) and the core (Fe_3O_4). Determination of thickness of the shell and overall size of the nanoparticles was done by statistical evaluation of 100 NPs. The thickness of the shell was found to be in the range of 35 ± 5 nm and overall size of the nanoparticles was in the range of 55 ± 10 nm. The functional groups present on the $\text{Fe}_3\text{O}_4@\text{SiO}_2\text{-NH}_2$ were characterized by FT-IR

spectroscopy (Figure 2C). The bands at 564 cm^{-1} , 796 cm^{-1} and 1097 cm^{-1} are assigned respectively for Fe-O stretching [54], Si-O-Si symmetrical and asymmetrical stretching [54]. The bands at 670 cm^{-1} (N-H wag), 1617 cm^{-1} (N-H bending) and the broad band centered at 3300 cm^{-1} presence of amine groups on the surface of $\text{Fe}_3\text{O}_4@\text{SiO}_2\text{-NH}_2$ [55]. Such surface functionalized Fe_3O_4 MNPs have also exhibited potent applications in theranostic as well as drug delivery applications [56].

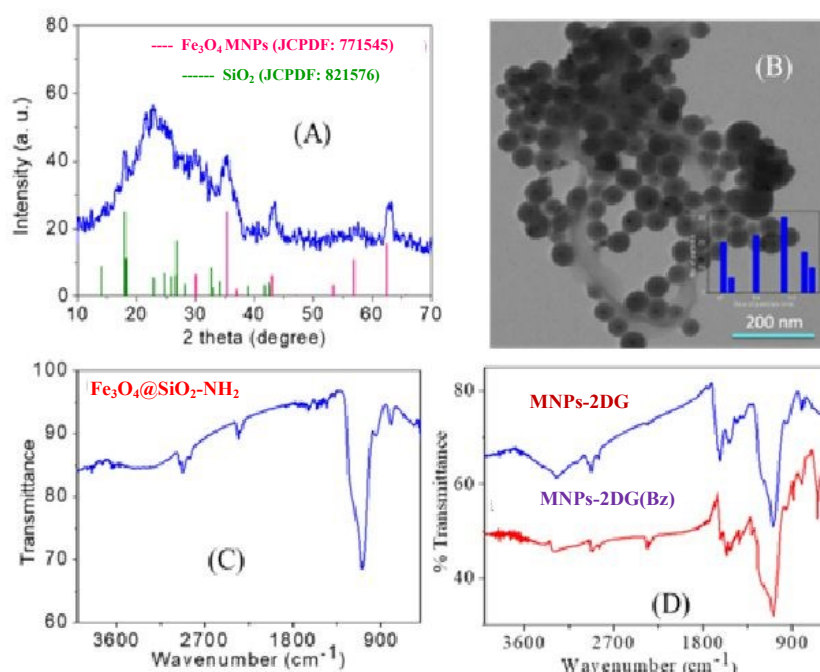
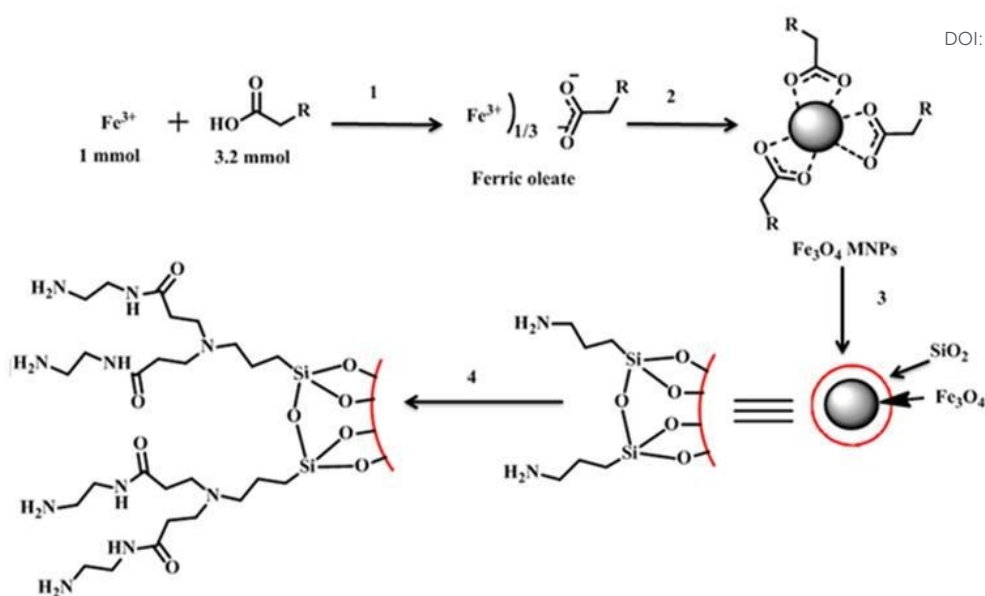


Figure 2. Characterization of $\text{Fe}_3\text{O}_4@\text{SiO}_2$ MNPs by XRD (2A), TEM (2B) and $\text{Fe}_3\text{O}_4@\text{SiO}_2\text{-NH}_2$ by FT-IR (2C); MNPs-2DG and MNPs-2DG-(Bz) (2D)

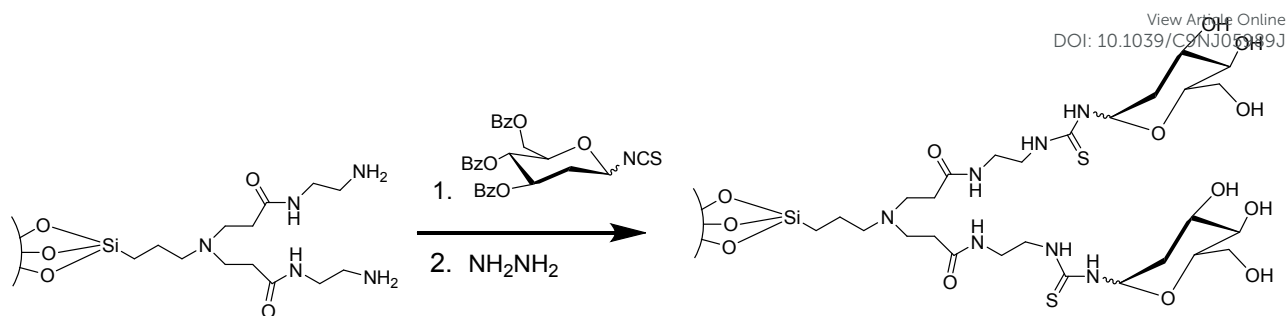
To increase the loading capacity of prodrug quantity of amine groups on the surface of the nanoparticles was increased by treating them with methyl acrylate followed by ethylenediamine [57]. The whole process was repeated three times and the amount of the amine groups was found to be enhanced ten times of the $\text{Fe}_3\text{O}_4@\text{SiO}_2\text{-NH}_2$ (Please see 2.2.2.). The resultant species MNPs-PAMAM (Scheme 1) were characterized with FT-IR spectroscopy.



Scheme 1. Synthesis of Fe₃O₄ MNPS and MNPs-PAMAM

(1: aq. MeOH solution and petroleum ether / aq. NaOH, oleic acid at RT (1 h), reflux (1 h); 2: in 1-octadecene at 320 °C (30 min) ; 3: in cyclohexane, aq. NH₃, Igepal-500, TEOS (74 h) and APTES (24 h); 4: methyl acrylate, ethylenediamine (at 0 °C), then at 45 °C (24 h).

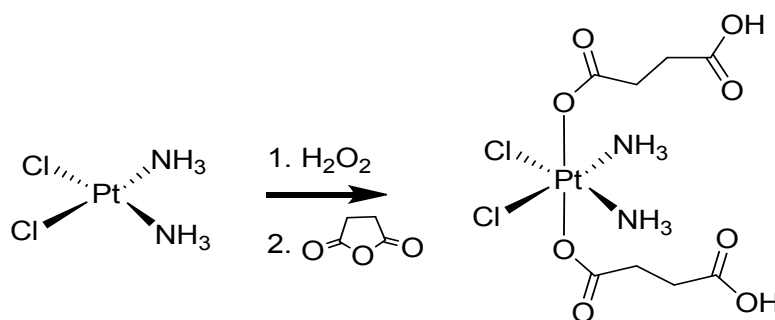
Further the loading of 2DG [58] was done by thiourea bond that was formed by the reacting amine groups [59] on the surface of the nanoparticles and isothiocyanate group of 3, 4, 5-tri-O-benzoyl-2-deoxyglycopyranosyl isothiocyanate. The synthesis of 3, 4, 5-tri-O-benzoyl-2-deoxyglycopyranosyl isothiocyanate was done by following the synthesis procedure as given in the procedures (Suppl. Info. Synthesis Procedures S 1: Glucose precursor). The conjugation of 3, 4, 5-tri-O-benzoyl-2-deoxyglycopyranosyl isothiocyanate with the amine functional groups was done by treating it with the nanoparticles dispersed in dried dimethylformamide (DMF) and heating at 60 °C for 6 h. The benzoyl protecting groups were removed by reacting with hydrazine hydrochloride in ethanol at 0 °C [60] (Scheme 2). The nanoparticles were characterized with FT-IR spectroscopy (Figure 2 D).



Scheme 2. Conjugation of MNPs-PAMAM with 2DG by reacting 3, 4, 5-tri-O-benzoyl-2-deoxyglycopyranosyl isothiocyanate (**1**) with the amine groups of MNPs-PAMAM and deprotection of benzoyl protecting groups by hydrazine hydrochloride (**2**).

The peak observed at 1652 cm^{-1} correspond to C=O stretching of amide of PAMAM. The peaks at 696, 967, 1396, 1448 and 1535 cm^{-1} are attributable to C=S stretching and bending of thiourea linkage formed between 2-deoxy-D-glucose isothiocyanate. The broad peak observed at 3289 cm^{-1} corresponds to the amine group of amide and O-H stretching vibrations of MNPs-2DG (Figure 2D). Band in region $3500\text{-}3200\text{ cm}^{-1}$ corresponds to the hydrogen bonds associated between neighbouring hydroxyl groups. The pyranose ring skeletal vibrations bands are represented by $990\text{-}840\text{ cm}^{-1}$ region. The intensive bands in $1384\text{-}1250\text{ cm}^{-1}$ region correspond to deformation vibration of hydroxyl group. The presence of these peaks on FT-IR spectra of MNPs-(benzoyl)-2DG and MNPs-2DG (Figure 2D) confirms the presence of 2DG moieties on the surface of MNPs. Further, the presence of 2-DG moiety on the surface of the MNPs-2DG was confirmed by treating ConA labeled with FITC [61]. With the increase in the amount of MNPs-2DG added to the fixed volume of the solution of Con A (1 mM) followed by measuring fluorescent intensity of the supernatant. A decrease in fluorescent intensity in accordance with the amount of MNPs-2DG was observed. (Suppl. Info. Figure S 11) This reveals that Con A was adsorbed on surface of MNPs-2DG

due to the interaction of Con A moiety with 2DG on the surface of the nanoparticles. Once the MNPs-2DG formulation was ready, the kinetically inert Pt(IV) prodrug of cisplatin [62] was prepared by oxidation of cisplatin with hydrogen peroxide by following the literature procedure (Scheme 3). The Pt(II) metal centre of cisplatin was oxidized to Pt(IV) by using H_2O_2 , generating two axial hydroxyl groups which was further made to react with succinic anhydride and formed two additional carboxyl groups [63]. The synthesized Pt(IV) prodrug of cisplatin was characterized by NMR (^1H , $^{13}\text{C}\{^1\text{H}\}$, $^{195}\text{Pt}\{^1\text{H}\}$) spectroscopy (Suppl. Info. Figures S 12-14).



Scheme 3. Synthesis of Pt(IV) prodrug of cisplatin by oxidizing cisplatin by H_2O_2 and further reaction of the axial hydroxyl groups with succinic anhydride

After achieving the pure Pt(IV) prodrug, the lability of axial groups *i.e.*, reduction was evaluated at an acidic pH (6.5) as well as a physiological pH (7.4) by cyclic voltammetry since it is well established that the cancerous cells have acidic environment due to formation of lactic acid as the end product during glycolysis. Hence it was anticipated that the axial ester groups should preferentially reduce in acidic pH conditions. The cyclic voltammetric studies show that maximum reduction of axial ester groups occur under acidic conditions as depicted in Figure 3 [64].

The redox potential for reduction of the Pt(IV) prodrug of cisplatin at pH 6.5 and 7.4 unit values was evaluated. These electrochemical analyses revealed that the prodrug exhibited an irreversible cyclic voltammetric response for the Pt(IV) / Pt(II) couple near -1.00 V vs.

Ag/AgCl in PBS buffer 1:10 mixture of compound solution in PBS buffer at pH 6.5 while relatively very less reduction at -1.20 V at pH 7.4 respectively at scanning rate of 30 mV.s⁻¹ (Figure 3). These reduction potentials are indicative that the prodrug is amply stable towards reduction in the bloodstream throughout delivery to the target cancer cells by the nanoparticles.

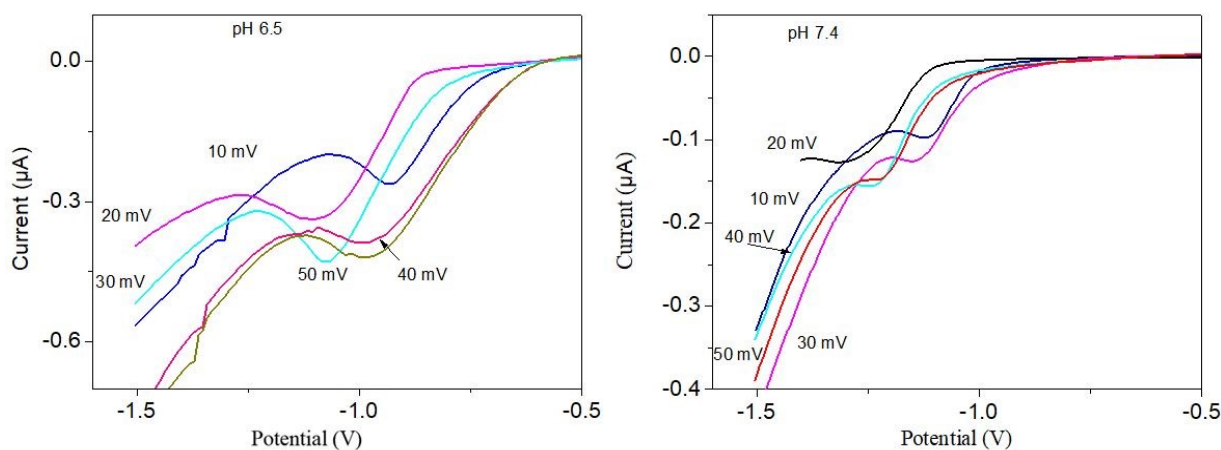
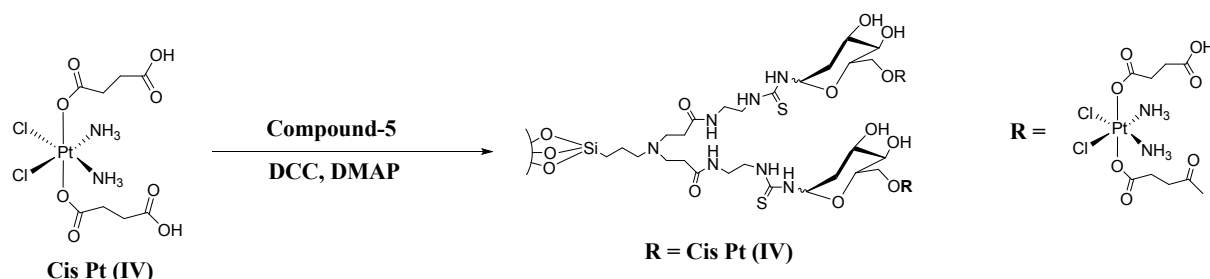


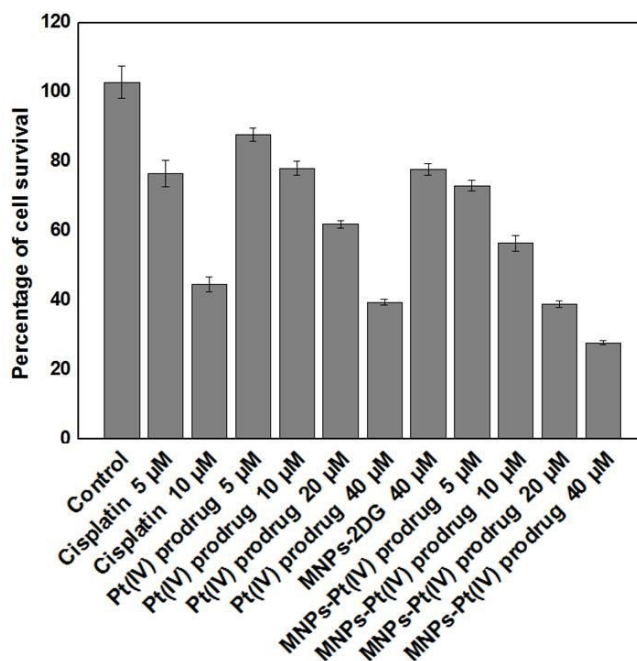
Figure 3. Cyclic voltammetry of 1.0 mM Pt(IV) prodrug of cisplatin in PBS buffer solution using Ag/AgCl with different scan rates of 10, 20, 30, 40, 50 mV s⁻¹ indicating variation of peak current of the first oxidation peak with the square root of the scan rates.

Loading of prodrug of cisplatin on MNPs-2DG was performed by well-known process of DCC coupling [65]. The activation of carboxylic groups of Pt(IV) prodrug was performed by N, N'-Dicyclohexylcarbodiimide (DCC) followed by its treatment with MNPs-2DG in DMF solvent at room temperature (Scheme 4) leading to ester bond formation between hydroxyl groups on the surface of MNPs-2DG and carboxyl groups of Pt(IV) prodrug. It is the desired formulation. The loading efficiency of Pt(IV) prodrug of cisplatin loaded on the surface of the nanoparticles was found to be 90 % which was quantified by ICP-OES analysis.



Scheme 4: Loading of Pt(IV) prodrug over surface functionalized Fe₃O₄ MNPs

This MNPs-Pt(IV) prodrug formulation was evaluated for its cytotoxicity *in vitro* against MCF-7 cell lines by MTT assay. The cytotoxicity of Pt(IV) prodrug of cisplatin, MNPs-2DG and MNPs-Pt(IV) prodrug prodrug was compared with the cisplatin. Cytotoxicity was evaluated against MCF-7 human breast cancer cell lines by treating with various concentrations of all test compounds and formulation at 5, 10, 20 and 40 μM concentrations (Figure 4). The IC₅₀ value of cisplatin has been observed to be 10 μM while the Pt(IV) prodrug exhibited IC₅₀ value of $\sim 30 \mu\text{M}$ which is indicative of kinetic inertness of Pt(IV) derivative as anticipated. This also demonstrates that the carrier MNPs-2DG exhibited negligible cytotoxicity. The 2DG itself has IC₅₀ of 10 milli-molar (mM). Since the loading of 2DG molecules over MNPs-2DG is in small amount, it does not contribute much to cytotoxicity. The formulation MNPs-Pt(IV) prodrug exhibited IC₅₀ of $\sim 14 \mu\text{M}$. Although the IC₅₀ value of prodrug is approximately triple than that of cisplatin, it is anticipated that the prodrug will be less toxic due to its kinetic inertness as a result of the octahedral structure. Hence, the present formulation will help to enhance the activity of prodrug of the cisplatin with reduced side effects. Due to the presence of 2DG, the above-mentioned formulation is supposed to be target specific, an aspect which needs to be checked in a subsequent work. It revealed the potency of formulation as observed IC₅₀ $\sim 14 \mu\text{M}$.



View Article Online
DOI: 10.1039/C9NJ05989J

Figure 4. MTT assay for treatment of MCF-7 cell lines with cisplatin, its prodrug and formulation

After initial evaluation of percentage cytotoxicity by MTT, we extended the cytotoxicity studies further to estimate the percentage of viable, apoptotic and dead cells by flow cytometric studies. Accordingly the evaluations on CHO, Colo-205 and MCF-7 cell lines treated with 10 μM solutions of cisplatin, Pt(IV) prodrug and corresponding concentrations of MNPs-2DG and MNPs-Pt(IV) prodrug were performed by using flow cytometer as shown in Table 1. Percentage viability, control, 10 μM Pt(IV) prodrug treated and 10 μM MNPs-2DG treated CHO cell lines were respectively 86.93 ± 0.87 , 89.52 ± 1.03 and 86.21 ± 0.22 . These values suggest the non-toxicity of Pt(IV) prodrug and our formulation, MNPs-2-DG. The values of percentage viability in case of cisplatin and MNPs-Pt(IV) prodrug were respectively 59.35 ± 3.28 and 50.67 ± 4.22 which show their similar activity. Values of percentage viability for Colo-205 cell lines treated with 10 μM solutions of cisplatin, Pt(IV) prodrug and corresponding concentrations of MNPs-2DG and MNPs-Pt(IV) prodrug are 76.1 ± 1.41 , 66.6 ± 3.54 , 64.87 ± 3.7 , 74.2 ± 0.14 and 63.73 ± 2.29 .

Similarly values of MCF-7 cell lines are respectively 75.235 ± 2.58 , 66.98 ± 3.07 , 66.1 ± 2.84 , 69.77 ± 6.93 and 45.37 ± 4.0 . Overall, the cytotoxic effect desired to kill cancer cells were observed with the current formulation as seen in treatment of MCF-7 and COLO 205 cell lines. The cytotoxic effect was however also observed in the normal CHO cell line. A possible explanation to this is the fusion of internalisation-efficient MNPs-Pt(IV) prodrug with lysosomes within cells. The acidic condition within lysosomes might have activated the MNPs-Pt(IV) prodrug which eventually exert its cytotoxic effect in subsequent cell cycles. Another possible explanation include the lesser DNA or chromosome content per cell. CHO cells typically contain 22 chromosomes compared to COLO 205 or MCF-7 which typically contain 46 chromosomes. The intercalation frequency of internalisation-efficient MNPs-Pt(IV) prodrug to DNA within CHO cells must likely be higher compared to COLO 205 and MCF-7 cells. Lower percentage viability of Cisplatin treated CHO cells compared to Cisplatin treated COLO 205 and MCF-7 cells (Please see the details in Suppl. Info. Table S 1, Figures S 15-19) support this assumption. The reduction of cytotoxicity to normal cells without compromising efficiency to kill cancer cells need to be studied deeper in future.

Table1. Cell toxicity studies on CHO, Colo-205 and MCF-7 cell lines in the presence of 10 μM of respective drugs and corresponding concentrations of MNPs-2DG and MNPs-Pt(IV) prodrug

Percentage viability of Cell lines	Control	Prodrug	Cisplatin	MNPs-2DG	MNPs-Pt(IV) prodrug
CHO	86.93 ± 0.87	89.52 ± 1.03	59.35 ± 3.28	86.21 ± 0.22	50.67 ± 4.22
Colo-205	76.1 ± 1.41	66.6 ± 3.54	64.87 ± 3.7	74.2 ± 0.14	63.73 ± 2.29
MCF-7	75.235 ± 2.58	66.98 ± 3.07	66.1 ± 2.84	69.77 ± 6.93	45.37 ± 4.0

After cytotoxicity studies it was worthwhile to assess the cellular uptake of the formulation. To study the higher intracellular uptake of MNPs-2DG in MCF-7 cells, MNPs-

 1
2
3
4
5
6
7
8
9
10
11
12
13
14
15
16
17
18
19
20
21
22
23
24
25
26
27
28
29
30
31
32
33
34
35
36
37
38
39
40
41
42
43
44
45
46
47
48
49
50
51
52
53
54
55
56
57
58
59
60

2DG were labeled with a fluorescent dye (fluorescein iso-thiocyanate, FITC), followed by treatment of MCF-7 cells with 400 μ l of MNPs-2DG-FITC. The cells were visualized by fluorescence microscopy where green fluorescence is observed in the cytoplasm and near the surface of the cells. The nucleus stained with DAPI didn't show co-localization with MNPs-2DG-FITC as observed in the merged image (Figure 5) suggesting that the MNPs are localized mainly in the cytoplasm and cell surface within 3 h. It exhibited efficient cellular uptake of test MNPs-2DG. In this case, the organic moiety attached at axial position of Pt(IV) prodrug of cisplatin tunes the lipophilicity of the prodrug, consequently improving the ability of the compound to accumulate into cancer cells

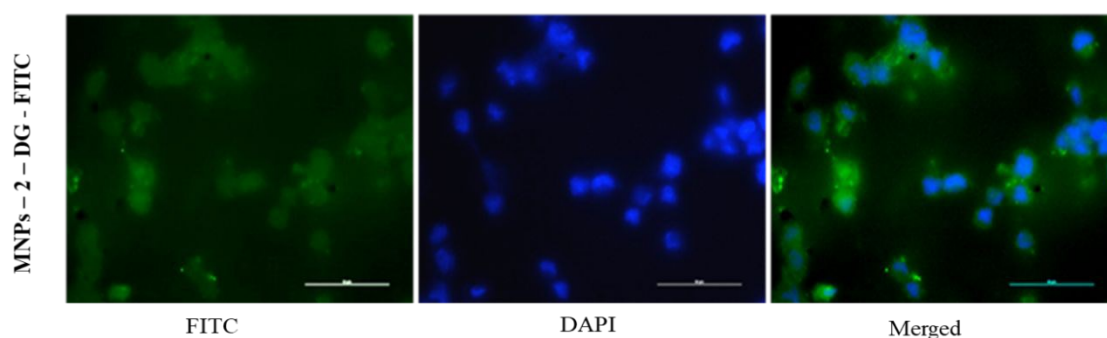


Figure 5. Fluorescence microscopy images of MCF-7 cells after treatment with MNPs-2DG-FITC. Nucleus is stained with DAPI (blue) and green color indicates MNPs-2DG labeled with FITC. Scale bar: 10 μ m.

The cellular uptake leads to internalization and eventually cell killing which are in correlation. As discussed earlier the flow cytometric evaluations have exhibited substantial percentage of apoptotic cells. It's well established that appearance of apoptosis has been recognized as an outcome of DNA damage. Literature reports have clearly stated about cisplatin, Pt(IV) prodrugs internalize in cell through Pt-DNA binding through covalent bond which induce the DNA damage leading to cancer cell death by triggering apoptotic pathway. Hence, the DNA binding ability of Pt compounds correlates with its ability to induce apoptosis [66]. In our case, from cyclic voltammetric studies, it's clear that Pt(IV) prodrug of cisplatin

was reduced to active form Pt(II) *i.e.*, cisplatin in acidic pH similar in cancer cells. Hence it reveals that that in cell the cisplatin was formed which binds with DNA leading to DNA damage which induced apoptosis and eventually cell death. This phenomenon of Pt compound-induced cell death should helpful in the development of more effective therapeutic strategies for the treatment of cancer.

Additionally the formulation was evaluated for heating effect under AC magnetic field [35]. For typical demonstration of heating efficacy, Fe₃O₄ particles coated with SiO₂ are dispersed in water; and the dispersed particles (5 or 10 mg per 1 ml) are kept in induction coil (frequency = 265 kHz, current = 400 A). 0.5 mg/ml of Fe₃O₄ particles produce 31-33 °C within 600 seconds at 400 A (335 Oe) (Figure 6) but could not reach hyperthermia temperature (*HT* = 42 °C). Similarly, 1 mg/ml particles at 400 A could not reach *HT*. But, 2 mg/ml at 400 A could reach *HT* in 1200 s.

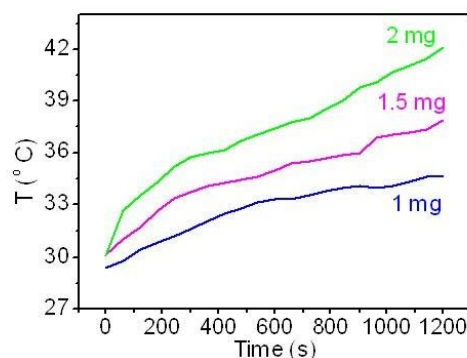


Figure 6: The evaluation of heat released with respect to time under AC magnetic field.

Specific absorption rates (SAR) of particles with concentrations of 0.5 mg / ml, 1 mg/ml, 2 mg/ml and 5 mg/ml are found to be 2.09, 3.26 and 4.96 W.g⁻¹, respectively and here, SAR is expressed in term of Watts per 1 g of Fe₃O₄. The heat generation from magnetic fluid under AC magnetic field comes from relaxation phenomena and hysteresis loop. Relaxation phenomena include Brownian motion of particles with liquid medium and single domain relaxation (10⁻⁵-10⁻¹⁰ s⁻¹) and hysteresis loss arises during AC frequency (265 kHz)

and applied magnetic field. Relaxation phenomena are dominating factor in case of smaller particles sizes, whereas hysteresis loss is dominating factor in case of bigger particles

4. Conclusions

In the present study, monodispersed, water dispersible Fe_3O_4 MNPs coated with silica (SiO_2) were synthesized. The SiO_2 surface was functionalized with poly(amidoamines) (PAMAM) which in turn conjugated with 2DG through thiourea bond formation. Further the 2DG was linked with Pt(IV) prodrug of cisplatin through the ester bond to afford the formulation. Here the silica coating and 2DG linking render the water dispersibility and biocompatibility to formulation. This formulation exhibited cytotoxicity against MCF-7 human breast cancer cell lines (IC_{50} value $\sim 14 \mu\text{M}$). Even though it is comparable to cell killing potency of cisplatin, the formulation is anticipated to exhibit reduced severe side effects of cisplatin. It was evidenced from the flow cytometric evaluations performed on MCF-7, Colo-205 cancer cells and CHO non-cancer cell. The MNPs-Pt(IV) prodrug is responsible to induce apoptosis in cancer cells evidenced from $\sim 30\%$ and $\sim 22\%$ of apoptotic cells in case of MCF-7 and COLO-205 cell lines respectively while only 3% for CHO cell lines for parental formulation. Further, the MNPs-2DG-FITC exhibited their efficient cell internalization in cytoplasm of MCF-7 cell lines within 3 h. It reveals the efficient and fast internalization of proposed formulation. It leads to conclusion that after the internalization, the Pt moiety from formulation interacts with DNA leading binding which leads to cell death through apoptotic pathway. Additionally the heating effect studies indicated that the formulation has the potential for hyperthermia applications also. The results divulge that the formulation is biocompatible and it is anticipated to be a competent pharmacological agent leading to further research for its clinical applications.

5. Supplementary information

View Article Online
DOI: 10.1039/C9NJ05989J

† Electronic supplementary information (ESI) available: The characterization data of Pt(IV) prodrug of cisplatin *viz.*, NMR (^1H , $^{13}\text{C}\{^1\text{H}\}$ and $^{195}\text{Pt}\{^1\text{H}\}$) and other experimental details like synthesis of 2-deoxy-D-glucose derivatives *etc.* are given in supplementary materials.

6. Acknowledgements

Authors are thankful to Dr. S. Kapoor Associate Director (D), Chemistry Group and Dr. A. K. Tyagi, Head, Chemistry Division, BARC, Trombay, Mumbai for the encouragement and support for this research work. Authors also acknowledge the fruitful discussions with Dr. R. S. Ningthoujam, Chemistry Division, BARC as well as Dr. Dibakar Goswami, Bio-Organic Division, BARC. KSS is grateful to University Grants Commission (UGC), New Delhi for the award of fellowship. The authors gratefully acknowledge help from Analytical Chemistry Division, BARC, for providing the cyclic voltammetry and ICP-OES analyses.

Author information

View Article Online
DOI: 10.1039/C9NJ05989J

Affiliations

Chemistry Division, Bhabha Atomic Research Centre, Mumbai, 400 085, India

K. Shitaljit Sharma

Chemistry Division, Bhabha Atomic Research Centre, Mumbai, 400 085, India &

Homi Bhabha National Institute, Anushaktinagar, Mumbai-400 094, India

Prasad P. Phadnis and Rajesh K. Vatsa

Bio-organic Division, Bhabha Atomic Research Centre, Mumbai, 400 085, India

Akhil K. Dubey

Radiopharmaceuticals Division, Bhabha Atomic Research Centre, Mumbai-400 085, India

Arunkumar S. Koijam and Chandan Kumar

Molecular Biology Division, Bhabha Atomic Research Centre, Mumbai-400 085, India

Anand Ballal

UGC-DAE Consortium for Scientific Research, Mumbai Centre, Mumbai-400 085, India

Sudip Mukherjee

Corresponding authors

Correspondence to: Dr. Prasad P. Phadnis; Dr. Rajesh K. Vatsa

Email: phadnisp@barc.gov.in; rkvatsa@barc.gov.in

Author contributions

View Article Online
DOI: 10.1039/C9NJ05989J

KSS and PPP designed the work and performed synthesis of silica coated Fe_3O_4 nanoparticles and Pt(IV) prodrug. KSS, AKD and PPP conducted the synthesis of glucose derivative and its functionalization with nanoparticles. SM performed magnetic measurements. AB performed TEM experiments. KSS evaluated the cell internalization of formulation as well as cytotoxicity against MCF-7 cancer cell lines by MTT assays. ASK and CK performed assessment of percentage viable, apoptotic and dead cells by flow cytometer. RKV supervised the experiments. KSS, PPP and RKV wrote the manuscript. All authors discussed the results and worked on the manuscript and approved the final version of manuscript.

Ethics declarations

Conflicts of interest

“There are no conflicts to declare”.

References

View Article Online
DOI: 10.1039/C9NJ05989J

- [1] B. Rosenberg, L. Van Camp, J. E. Trosko and V. H. Mansour, *Nature*, 1969, **222**, 385-386.
- [2] D. Wang and S. J. Lippard, *Nat. Rev. Drug Discov.*, 2005, **4**, 307-320.
- [3] R. Canetta, M. Rozenzweig and S. K. Carter, *Cancer Treat. Rev.*, 1985, **12**, 125-136; S. Dasari and P. B. Tchounwou, *Eur. J. Pharmacol.*, 2014, **0**, 364-378; A.-M. Florea and D. Büsselberg, *Cancers*, 2011, **3**, 1351-1371.
- [4] J. Sastry and S. J. Kellie, *Pediatr. Hematol. Oncol.*, 2005, **22**, 441-445; T. Karasawa and P. S. Steyger, *Toxicol. Lett.*, 2015, **237**, 219-227; L. P. Rybak, D. Mukherjia, S. Jajoo and V. Ramkumar, *Tohoku J. Exp. Med.*, 2009, **219**, 177-186.
- [5] G. Housman, S. Byler, S. Heerboth, K. Lapinska, M. Longacre, N. Snyder and S. Sarkar, *Cancers*, 2014, **6**, 1769-1792; B. Mansoori, A. Mohammadi, S. Davudian, S. Shirjang and B. Baradaran, *Adv. Pharm. Bull.*, 2017, **7**, 339-348.
- [6] M. D. Hall, H. R. Mellor, R. Callaghan and T. W. Hambley, *J. Med. Chem.*, 2007, **50**, 3403-3411; C. F. Chin, Q. Tian, M. I. Setyawati, W. Fang, E. S. Q. Tan, D. T. Leong and W. H. Ang, *J. Med. Chem.*, 2012, **55**, 7571-7582; M. D. Hall and T. W. Hambley, *Coord. Chem. Rev.*, 2002, **232**, 49-67.
- [7] A. Nemirovski, Y. Kasherman, Y. Tzaraf and D. Gibson, *J. Med. Chem.*, 2007, **50**, 5554-5556.
- [8] M. Ravera, E. Gabano, I. Zanellato, I. Bonarrigo, M. Alessio, F. Arnesano, A. Galliani, G. Natile and D. Osella, *J. Inorg. Biochem.*, 2015, **150**, 1-8; Y. Song, K. Suntharalingam, J. S. Yeung, M. Royzen and S. J. Lippard, *Bioconjugate Chem.*, 2013, **24**, 1733-1740.
- [9] E. Gabano, M. Ravera and D. Osella, *Dalton Trans.*, 2014, **43**, 9813-9820; D. Gibson, *Dalton Trans.*, 2016, **45**, 12983-12991.

- 1
2
3
4
5
6
7
8
9
10
11
12
13
14
15
16
17
18
19
20
21
22
23
24
25
26
27
28
29
30
31
32
33
34
35
36
37
38
39
40
41
42
43
44
45
46
47
48
49
50
51
52
53
54
55
56
57
58
59
60
- [10] S. Choi, C. Filotto, M. Bisanzo, S. Delaney, D. Lagasee, J. L. Whitworth, A. Jusko, C. Li, N. A. Wood, J. Willingham, A. Schwenker and K. Spaulding, *Inorg. Chem.*, 1998, **37**, 2500-2504. View Article Online
DOI: 10.1039/C9NJ05989J
- [11] E. Wexselblatt, E. Yavin and D. Gibson, *Angew. Chem. Int. Ed.*, 2013, **22**, 6059-6062.
- [12] A. A. Ammar, R. Raveendran, D. Gibson, T. Nassar and S. Benita, *J. Med. Chem.*, 2016, **59**, 9035-9046; I. Zanellato, I. Bonarrigo, D. Colangelo, E. Gabano, M. Ravera, M. Alessio and D. Osella, *J. Inorg. Biochem.*, 2014, **140**, 219-227; U. Basu, B. Banik, R. Wen, R. K. Pathak and S. Dhar, *Dalton Trans.*, 2016, **45**, 12992-13004.
- [13] V. Novohradsky, I. Zanellato, C. Marzano, J. Pracharova, J. Kasparkova, D. Gibson, V. Gandin, D. Osella and V. Brabec, *Sci. Rep.*, 2017, **7**, Article number: 3751 (P. 1-14); M. Alessio, I. Zanellato, I. Bonarrigo, E. Gabano, M. Ravera and D. Osella, *J. Inorg. Biochem.*, 2013, **129**, 52-57; M. Ravera, E. Gabano, I. Zanellato, F. Fregonese, G. Pelosi, J. A. Platts and D. Osella, *Dalton Trans.*, 2016, **45**, 5300-5309.
- [14] H. Tian, J. Dong, X. Chi, L. Xu, H. Shi and T. Shi, *Int. J. Chem. Kinet.*, 2017, **49**, 681-689.
- [15] G. Verma and P. A. Hassan, *Phys. Chem. Chem. Phys.*, 2013, **15**, 17016-17028; A. Anselmo and S. Mitragotri, *AIChE Journal*, 2016, 52-58; D. Lombardo, M. A. Kiselev and M. T. Caccamo, *J. Nanomater.*, 2019, **2019**, Article ID 3702518 (1-26 pages); S. Senapati, A. K. Mahanta, S. Kumar and P. Maiti, *Signal Transduct. Tar.*, 2018, **3**, 1-19; Y. Yang, X. Wang, G. Liao, X. Liu, Q. Chen, H. Li, L. Lu, P. Zhao and Z. Yu, *J. Colloid Interface Sci.*, 2018, **509**, 515-521.
- [16] Y. Yu, Q. Xu, S. He, H. Xiong, Q. Zhang, W. Xu, V. Ricotta, L. Bai, Q. Zhang, Z. Yu, J. Ding, H. Xiao and D. Zhou, *Coord. Chem. Rev.*, 2019, **387**, 154-179; C. Li, J. Wang, Y. Wang, H. Gao, G. Wei, Y. Huang, H. Yu, Y. Gan, Y. Wang, L. Mei, H. Chen, H. Hu, Z. Zhang and Y. Jin, *Acta Pharm. Sin. B*, 2019, **9**, 1145-1162; G.

- 1
2
3 Tiwari, R. Tiwari, B. Sriwastawa, L. Bhati, S. Pandey, P. Pandey and S. K. Bannerjee, *View Article Online*
4 *Int. J. Pharma. Investig.*, 2012, **2**, 2-11. DOI: 10.1055/C914J05989J
- 5
6
7
8 [17] H. A. Santos, L. M. Bimbo, L. Peltonen and J. Hirvonen, *Inorganic Nanoparticles in*
9 *Targeted Drug Delivery and Imaging*, Chapter 18 Pages 571-613, in *Targeted Drug*
10 *Delivery: Concepts and Design*, P. Devarajan and S. Jain (Eds.), Print ISBN 978-3-
11 319-11354-8 at Cham, Springer International Publishing AG, 2015; Y. Ghosn, M. H.
12 Kamareddine, A. Tawk, C. Elia, A. E. Mahmoud, K. Terro, N. E. Harake, B. E-Baba,
13 J. Makkessi and S. Farhat, *Technol. Cancer Res. Treat.*, 2019, **18**, 1-12.
- 14
15
16
17 [18] M.-X. Wu and Y.-W. Yang, *Adv. Mater.*, 2017, **29**, 1606134 (1-20); X.-G. Wang, Z.-
18 Y. Dong, H. Cheng, S.-S. Wan, W.-H. Chen, M.-Z. Zou, J.-W. Huo, H.-X. Deng and
19 X.-Z. Zhang, *Nanoscale*, 2015, **7**, 16061-16070; C. He, K. Lu, D. Liu and W. Lin, *J.*
20 *Am. Chem. Soc.*, 2014, **136**, 5181-5184.
- 21
22
23
24 [19] S. Gao, G. Tang, D. Hua, R. Xiong, J. Han, S. Jiang, Q. Zhang and C. Huang, *J.*
25 *Mater. Chem. B*, 2019, **7**, 709-729; P. Wu, X. Wang, Z. Wang, W. Ma, J. Guo, J.
26 Chen, Z. Yu, J. Li and D. Zhou, *ACS Appl. Mater. Inter.*, 2019, **11**, 18691-18700.
- 27
28
29
30 [20] A. Jain, S. K. Singh, S. K. Arya, S. C. Kundu, and S. Kapoor, *ACS Biomater. Sci.*
31 *Eng.*, 2018, **4**, 3939-3961; C. D. Spicer, C. Jumeaux, B. Gupta and M. M. Stevens,
32 *Chem. Soc. Rev.*, 2018, **47**, 3574-3620.
- 33
34
35
36 [21] Q. Chen, Y. Yang, X. Lin, W. Ma, G. Chen, W. Li, X. Wang and Z. Yu, *Chem.*
37 *Commun.*, 2018, **54**, 5369-5372.
- 38
39
40
41 [22] S. H. Medina and M. E. H. El-Sayed, *Chem. Rev.*, 2009, **109**, 3141-3157; A.-M.
42 Caminade and C.-O. Turrin, *J. Mater. Chem. B*, 2014, **2**, 4055-4066.
- 43
44
45
46 [23] J. S. Butler and P. J. Sadler, *Cur. Opin. Chem. Biol.*, 2013, **17**, 175-188; P. Ma, H.
47 Xiao, C. Li, Y. Dai, Z. Cheng, Z Hou and J. Lin, *Mater. Today*, 2015, **18**, 554-564.
- 48
49
50
51
52
53
54
55
56
57
58
59
60

- 1
2
3 [24] D. Li, M. Deng, Z. Yu, W. Liu, G. Zhou, W. Li, X. Wang, D.-P. Yang and W. Zhang, *ACS Biomater. Sci. Eng.*, 2018, **4**, 2143-2154; E.-K. Lim, T. Kim, S. Paik, S. Haam,
4 *ACS Biomater. Sci. Eng.*, 2018, **4**, 2143-2154; E.-K. Lim, T. Kim, S. Paik, S. Haam,
5 *ACS Biomater. Sci. Eng.*, 2018, **4**, 2143-2154; E.-K. Lim, T. Kim, S. Paik, S. Haam,
6 *ACS Biomater. Sci. Eng.*, 2018, **4**, 2143-2154; E.-K. Lim, T. Kim, S. Paik, S. Haam,
7 Y.-M. Huh and K. Lee, *Chem. Rev.*, 2015, **115**, 327-394; J. Xie, S. Lee and X. Chen,
8 *Chem. Rev.*, 2015, **115**, 327-394; J. Xie, S. Lee and X. Chen,
9 *Chem. Rev.*, 2015, **115**, 327-394; J. Xie, S. Lee and X. Chen,
10 *Adv. Drug Deliv. Rev.*, 2010, **62**, 1064-1079.
11
12 [25] G. Kandasamy, A. Sudame, T. Luthra, K. Saini and D. Maity, *ACS Omega*, 2018, **3**,
13 3991-4005.
14
15 [26] P. Guardia, R. D. Corato, L. Lartigue, C. Wilhelm, A. Espinosa, M. Garcia-
16 Hernandez, F. Gazeau, L. Manna and T. Pellegrino, *ACS Nano*, 2012, **6**, 3080-3091;
17 J. Kolosnjaj-Tabi, R. D. Corato, L. Lartigue, I. Marangon, P. Guardia, A. K. A. Silva,
18 N. Luciani, O. Clément, P. Flaud, J. V. Singh, P. Decuzzi, T. Pellegrino, C. Wilhelm
19 and F. Gazeau, *ACS Nano*, 2014, **8**, 4268-4283; A. Hofmann, S. Thierbach, A.
20 Semisch, A. Hartwig, M. Taupitz, E. Rühl and C. Graf, *J. Mater. Chem.*, 2010, **20**,
21 7842-7853.
22
23 [27] N. Singh, S. K. Sahoo and R. Kumar, *Mater. Sci. Eng. C*, 2020, **109**, 10645 (1-10
24 pages); Y. P. Yew, K. Shameli, M. Miyake, N. B. B. A. Khairudin, S. E. B.
25 Mohamad, T. Naiki and K. X. Lee, *Arab. J. Chem.*, 2020, **13**, 2287-2308.
26
27 [28] A. M. Maharramov, M. A. Ramazanov, A. I. Ahadova, M. Kloor, J. Kopitz, M. V. K.
28 Doeberitz, A. L. Shabanov, Q. M. Eyvazova, Z. A. Agamaliyev, F. V. Hajiyeva, S. B.
29 Veliyeva and U. A. Hasanova, *Dig. J. Nanomater. Bios.*, 2014, **9**, 1461-1469 and
30 references therein.
31
32 [29] H. Xi, M. Kurtoglu and T. J. Lampidis, *IUBMB Life*, 2014, **66**, 110-121; R. L. Aft, F.
33 W. Zhang and D. Gius, *Brit. J. Cancer*, 2002, **87**, 805-812.
34
35 [30] M. V. Liberti and J. W. Locasale, *Trends Biochem. Sci.*, 2016, **41**, 211-218; A. M.
36 Otto, *Cancer Metab.*, 2016, **4**, 1-8.
37
38
39
40
41
42
43
44
45
46
47
48
49
50
51
52
53
54
55
56
57
58
59
60

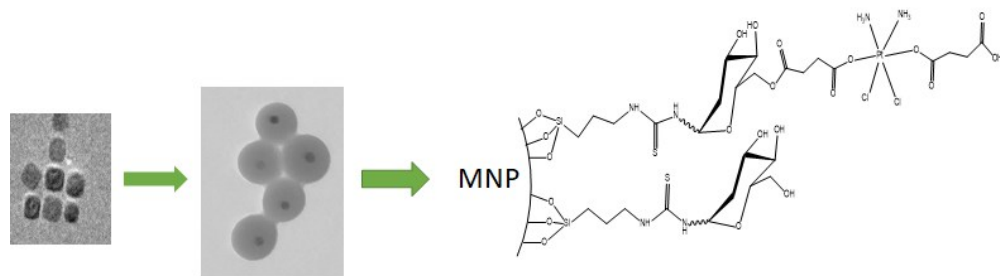
- 1
2
3
4
5
6
7
8
9
10
11
12
13
14
15
16
17
18
19
20
21
22
23
24
25
26
27
28
29
30
31
32
33
34
35
36
37
38
39
40
41
42
43
44
45
46
47
48
49
50
51
52
53
54
55
56
57
58
59
60
- [31] S. T. Selvan, P. K. Patra, C. Y. Ang and J. Y. Ying, *Angew. Chem. Int. Ed.*, 2007, **46**, 2448-2452; D. K. Yi, S. T. Selvan, S. S. Lee, G. C. Papaefthymiou, D. Kundaliya and J. Y. Ying, *J. Am. Chem. Soc.*, 2005, **127**, 4990-4991.
- [32] W. Wu, Z. Wu, T. Yu, C. Jiang and W.-S. Kim, *Sci. Technol. Adv. Mater.*, 2015, **16**, 023501 (1-43 pages); J. Gao, X. Ran, C. Shi, H. Cheng, T. Cheng and Y. Su, *Nanoscale*, 2013, **5**, 7026-7033; C. Xu and S. Sun, *Polym. Internat.*, 2007, **56**, 821-826.
- [33] A. M. Akbarzadeh, M. Samiei and S. Davaran, *Nanoscale Res. Lett.*, 2012, **7**, 1-13.
- [34] W. L. F. Armarego and D. D. Perrin, *Purification of Laboratory Chemicals*, Pergamon, Oxford, 4th Edn. 1996.
- [35] K. S. Sharma, R. S. Ningthoujam, A. K. Dubey, A. Chattopadhyay, S. Phapale, R. R. Juluri, S. Mukherjee, R. Tewari, N. G. Shetake, B. N. Pandey and R. K. Vatsa, *Sci. Rep.*, 2018, **8**, Article number: 14766 (P 1-11).
- [36] H. Singh, J. K. Rajput, P. Arora and Jigyasa, *RSC Adv.*, 2016, **6**, 84658-84671.
- [37] Y. Shi, S.-A. Liu, D. J. Kerwood, J. Goodisman and J. C. Dabrowiak, *J. Inorg. Biochem.*, 2012, **107**, 6-14.
- [38] T. Mosmann, *J. Immunol. Methods*, 1983, **65**, 55-63.
- [39] L. Jiang, R. Tixeira, S. Caruso, G. K. Atkin-Smith, A. A Baxter, S. Paone, M. D. Hulett and I. K. H. Poon, *Nat. Protoc.*, 2016, **11**, 655-663; N. M. Brown, S. M. Martin, N. Maurice, T. Kuwana and C. M. Knudson, *J. Biol. Chem.*, 2007, **282**, 2144-2155; T. A. Mansoor, P. M. Borralho, X. Luo, S. Mulhovo, C. M. P. Rodrigues and M.-J. U. Ferreira, *J. Nat. Prod.*, 2014, **77**, 1825-1830.
- [40] J. He, Y. Zhang, Q. Yuan and H. Liang, *Ind. Eng. Chem. Res.*, 2019, **58**, 3555-3560.

- 1
2
3 [41] M. Rahimi, K. D. Safa, E. Alizadeh and R. Salehi, *New J. Chem.*, 2017, **41**, 3177-3189; J. Barar, V. Kafil, M. H. Majd, A. Barzegari, S. Khani, M. Johari-Ahar, D.
4 3189; J. Barar, V. Kafil, M. H. Majd, A. Barzegari, S. Khani, M. Johari-Ahar, D.
5 Asgari, G. Cokous and Y. Omid, *J. Nanobiotechnol.*, 2015, **13**, (1-16 pages).
6
7
8
9
10 [42] V. M. Khot, A. B. Salunkhe, J. M. Ruso and S. H. Pawar, *J. Magn. Magn. Mater.*,
11 2015, **384**, 335-343.
12
13
14 [43] R. Hufschmid, H. Arami, R. M. Ferguson, M. Gonzales, E. Teeman, L. N. Brush, N.
15 D. Browning and K. M. Krishnan, *Nanoscale*, 2015, **7**, 11142-11154.
16
17
18 [44] R. Yuvakkumar and S. I. Hong, *Adv. Mater. Res.*, 2014, **1051**, 39-42; M. Das, D.
19 Mishra, T. K. Maiti, A. Basak and P. Pramanik, *Nanotechnology*, 2008, **19**, 415101
20 (1-14); S. Y. Unsoy, R. Khodadust, G. Gunduz and U. Gunduz, *J. Nanopart. Res.*,
21 2012, **14**, 1-13.
22
23
24 [45] E. Huseynov, A. Garibova and R. Mehdiyevab, *Mater. Res. Technol.*, 2016, **5**, 213-
25 218; S. R. Byrn, G. Zografı and X. (Sean) Chen, *Solid-State Properties of*
26 *Pharmaceutical Materials*, ISBN: 9781119264453, John Wiley & Sons Inc. USA,
27 2017; M. A. Asadabad and M. J. Eskandari, *Synth. React. Inorg. M.*, 2015, **45**, 323-
28 326; W. D. Pyrz and D. J. Buttrey, *Langmuir*, 2008, **24**, 11350-11360.
29
30
31 [46] Z. L. Liu, Y. J. Liu, K. L. Yao, Z. H. Ding, J. Tao and X. Wang, *J. Mater. Synth.*
32 *Process.*, 2002, **10**, 83-87; I. Karimzadeh, M. Aghazadeh, T. Doroudi, M. R. Ganjali
33 and P. H. Kolivand, *Adv. Phys. Chem.*, 2017, **2017**, Article ID 9437487 (1-7 pages).
34
35
36 [47] M. Mahmoudi, H. Hofmann, B. Rothen-Rutishauser and A. Petri-Fink, *Chem. Rev.*,
37 2012, **112**, 2323-2338; K. R. Wierzbinski, T. Szymanski, N. Rozwadowska, J. D.
38 Rybka, A. Zimna, T. Zalewski, K. Nowicka-Bauer, A. Malcher, M. Nowaczyk, M.
39 Krupinski, M. Fiedorowicz, P. Bogorodzki, P. Grieb, M. Giersig and M. K. Kurpisz,
40 *Sci. Rep.*, 2018, **8**, 3682 (1-17 pages); N. Lee, D. Yoo, D. Ling, M. H. Cho, T. Hyeon
41 and J. Cheon, *Chem. Rev.*, 2015, **115**, 10637-10689.
42
43
44
45
46
47
48
49
50
51
52
53
54
55
56
57
58
59
60

- 1
2
3
4
5
6
7
8
9
10
11
12
13
14
15
16
17
18
19
20
21
22
23
24
25
26
27
28
29
30
31
32
33
34
35
36
37
38
39
40
41
42
43
44
45
46
47
48
49
50
51
52
53
54
55
56
57
58
59
60
- [48] M. Qi, K. Zhang, S. Li, J. Wu, C. Pham-Huy, X. Diao, D. Xiao and H. He, *New J. Chem.*, 2016, **40**, 4480-4491; Z. Ferjaoui, R. Schneider, A. Meftah, E. Gaffet and H. Alem, *RSC Adv.*, 2017, **7**, 26243-26249.
- [49] T. Sadhukha, L. Niu, T. S. Wiedmann and J. Panyam, *Mol. Pharmaceutics*, 2013, **10**, 1432-1441; Y.-K. Huang, C.-H. Su, J.-J. Chen, C.-T. Chang, Y.-H. Tsai, S.-F. Syu, T.-T. Tseng and C.-S. Yeh, *ACS Appl. Mater. Interfaces*, 2016, **8**, 14470-14480.
- [50] L. H. Reddy, J. L. Arias, J. Nicolas and P. Couvreur, *Chem. Rev.*, 2012, **112**, 5818-5878; U. O. Häfeli, J. S. Riffle, L. Harris-Shekhawat, A. Carmichael-Baranauskas, F. Mark, J. P. Dailey and D. Bardenstein, *Mol. Pharmaceutics*, 2009, **6**, 1417-1428; X. F. Zhang, S. Mansouri, D. A. Mbeh, L. H. Yahia, E. Sacher and T. Veres, *Langmuir*, 2012, **28**, 12879-12885.
- [51] H. Xu, L. Cui, N. Tong and H. Gu, *J. Am. Chem. Soc.*, 2006, **128**, 15582-15583.
- [52] A.-L. Morel, S. I. Nikitenko, K. Gionnet, A. Wattiaux, J. Lai-Kee-Him, C. Labrugere, B. Chevalier, G. Deleris, C. Petibois, A. Brisson and M. Simonoff, *ACS Nano.*, 2008, **2**, 847-856; A. K. Gupta and M. Gupta, *Biomaterials*, 2005, **26**, 3995-4021.
- [53] W. Stöber, A. Fink and E. Bohn, *J. Colloid Interface Sci.*, 1968, **26**, 62-69.
- [54] F. Ahangaran, A. Hassanzadeh and S. Nouri, *Int. Nano Lett.*, 2013, **3**, 23-27.
- [55] G. Fang, H. Chen, Y. Zhang and A. Chen, *Int. J. Biol. Macromol.*, 2016, **88**, 189-195.
- [56] R. Ge, X. Li, M. Lin, D. Wang, S. Li, S. Liu, Q. Tang, Y. Liu, J. Jiang, L. Liu, H. Sun, H. Zhang and B. Yang, *ACS Appl. Mater. Interfaces*, 2016, **8**, 22942-22952; W. Chen, X. Wen, G. Zhen and X. Zheng, *RSC Adv.*, 2015, **5**, 69307-69311; I. Monaco, F. Arena, S. Biffi, E. Locatelli, B. Bortot, F. L. Cava, G. M. Marini, G. M. Severini, E. Terreno and M. C. Franchini, *Bioconjugate Chem.*, 2017, **28**, 1382-1390.
- [57] P. Zhao, L. Tian, X. Li, Z. Ali, B. Zhang, H. Zhang and Q. Zhang, *ACS Sustainable Chem. Eng.*, 2016, **4**, 6382-6390; M. A. Mees and R. Hoogenboom, *Macromolecules*,

- 2015, **48**, 3531-3538; H.-S. Jung, D.-S. Moon and J.-K. Lee, *J. Nanomater.* **2012**, Article ID 593471 (1-8 pages).
- [58] L. Zhao, Y. Zheng, H. Yan, W. Xie, X. Sun, N. Li and J. Tang, *J. Nanosci. Nanotechnol.*, 2016, **16**, 2401-2407; X.-H. Shan, P. Wang, F. Xiong, H.-Y. Lu and H. Hu, *Cancer Biomark.*, 2017, **18**, 367-374; J. Neamtu and N. Verga, *Dig. J. Nanomater. Bios.*, 2011, **6**, 969-978.
- [59] T. Maki, T. Tsuritani and T. Yasukata, *Org. Lett.*, 2014, **16**, 1868-1871.
- [60] R. Zerrouki, V. Roy, A. Hadj-Bouazza and P. Krausz, *J. Carbohydrate Chem.*, 2004, **23**, 299-303; W. A. Wlassoff, R. M. J. Finlay and C. J. Hamilton, *Synth. Commun.*, 2007, **37**, 2927-2934.
- [61] P. C. Pinheiro, A. L. Daniel-da-Silva, D. S. Tavares, M. P. Calatayud, G. F. Goya and T. Trindade, *Materials*, 2013, **6**, 3213-3225; A. K. Locke, B. M. Cummins, A. A. Abraham and G. L. Coté, *Anal. Chem.*, 2014, **86**, 9091-9097; Y. Zhang, S. W. Y. Gong, L. Jin, S. M. Li, Z. P. Chen, M. Ma and N. Gu, *Chin. Chem. Lett.*, 2009, **20**, 969-972; K. Sato and J. I. Anzai, *Anal. Bioanal. Chem.*, 2006, **384**, 1297-1301; R. J. Russell and M. V. Pishko, *Anal. Chem.*, 1999, **71**, 3126-3132.
- [62] T. C. Johnstone, K. Suntharalingam and S. J. Lippard, *Chem. Rev.*, 2016, **116**, 3436-3486; R. G. Kenny and C. J. Marmion, *Chem. Rev.*, 2019, **119**, 1058-1137.
- [63] R. Huang, Q. Wang, X. Zhang, J. Zhu and B. Sun, *Biomed. Pharmacother.*, 2015, **72**, 17-23; Y.-R. Zheng, K. Suntharalingam, T. C. Johnstone and S. J. Lippard, *Chem. Sci.*, 2015, **6**, 1189-1193.
- [64] S. Dhar, F. X. Gu, R. Langer, O. C. Farokhzad and S. J. Lippard, *PNAS*, 2008, **105**, 17356-17361.
- [65] E. Valeur and M. Bradley, *Chem. Soc. Rev.*, 2009, **38**, 606-631; C. A. G. N. Montalbetti and V. Falque, *Tetrahedron*, 2005, **61**, 10827-10852.

- 1
2
3 [66] Y. Sedletska, M.-J. Giraud-Panis and J.-M. Malinge, *Curr. Med. Chem. - Anti-Cancer* View Article Online
DOI: 10.1059/C9NJ05989J
4 *Agents*, 2005, **5**, 251-265; L. Gatti, R. Supino, P. Perego, R. Pavesi, C. Caserini, N.
5 Carenini, S. C. Righetti, V. Zuco and F. Zunino, *Cell Death Differ.*, 2002, **9**, 1352-
6 1359; H. Ye, C. Cande, N. C Stephanou, S. Jiang, S. Gurbuxani, N. Larochette, E.
7 Daugas, C. Garrido, G. Kroemer and H. Wu, *Nat. Struct. Biol.*, 2002, **9**, 680-684; A.
8 Basu and S. Krishnamurthy, *J. Nucleic Acids*, 2010, **2010**, Article ID 201367 (1-16
9 pages); C.-X. Yang, L. Xing, X. Chang, T.-J. Zhou, Y.-Y. Bi, Z.-Q. Yu, Z.-Q. Zhang
10 and H.-L. Jiang, *Mol. Pharm.*, 2020, **17**, 1300-1309; D. Montagner, D. Tolan, E.
11 Andriollo, V. Gandin and C. Marzano, *Int. J. Mol. Sci.*, 2018, **19**, 3775 (1-11 pages);
12 O. V. Blanářová, I. Jelínková, A. Szöör, B. Skender, K. Souček, V. Horváth, A.
13 Vaculová, L. Anděra, P. Sova, J. Szöllösi, J. Hofmanová, G. Vereb and A. Kozubík,
14 *Carcinogenesis*, 2011, **32**, 42-51; V. M. Gonzalez, M. A. Fuertes, C. Alonso and J. M.
15 Perwz, *Mol. Pharmacol.*, 2001, **59**, 657-663.
16
17
18
19
20
21
22
23
24
25
26
27
28
29
30
31
32
33
34
35
36
37
38
39
40
41
42
43
44
45
46
47
48
49
50
51
52
53
54
55
56
57
58
59
60



209x65mm (96 x 96 DPI)

1
2
3
4
5
6
7
8
9
10
11
12
13
14
15
16
17
18
19
20
21
22
23
24
25
26
27
28
29
30
31
32
33
34
35
36
37
38
39
40
41
42
43
44
45
46
47
48
49
50
51
52
53
54
55
56
57
58
59
60